Influence of the macroscopic shape of the tip on the contrast in scanning polarization force microscopy images

2009 Nanotechnology 20 285704

(http://iopscience.iop.org/0957-4484/20/28/285704)

Nanotechnology **20** (2009) 285704 (5pp) doi:10.1088/0957-4484/20/28/285704

Influence of the macroscopic shape of the tip on the contrast in scanning polarization force microscopy images

G M Sacha[1], M Cardellach[2], J J Segura[2], J Moser[2], A Bachtold[2], J Fraxedas[2] and A Verdaguer[2]

[1] Grupo de Neurocomputación Biológica Escuela Politécnica Superior, Universidad Autónoma de Madrid, Cantoblanco, Madrid, E-28049, Spain
[2] Centre d' Investigació en Nanociència i Nanotecnologia, CIN2 (CSIC-ICN), Esfera UAB, Campus de la UAB, Edifici CM-7, 08193-Bellaterra, Catalunya, Spain

Received 19 February 2009, in final form 30 April 2009
Published 24 June 2009
Online at stacks.iop.org/Nano/20/285704

Abstract

We demonstrate that a quantitative analysis of the contrast obtained in electrostatic force microscopy images that probe the dielectric response of the sample (scanning polarization force microscopy (SPFM)) requires numerical simulations that take into account both the macroscopic shape of the tip and the nanoscopic tip apex. To simulate the SPFM contrast, we have used the generalized image charge method (GICM), which is able to accurately deal with distances between a few nanometers and several microns, thus involving more than three orders of magnitude. Our numerical simulations show that the macroscopic shape of the tip accounts for most of the SPFM contrast. Moreover, we find a quasi-linear relation between the working tip–sample distance and the contrast for tip radii between 50 and 200 nm. Our calculations are compared with experimental measurements of the contrast between a thermally grown silicon oxide sample and a few-layer graphene film transferred onto it.

(Some figures in this article are in colour only in the electronic version)

1. Introduction

Electrostatic force microscopy (EFM) [1] has been used to designate different operational modes of scanning force microscopy (SFM) that probe electrostatic forces between a tip and a sample. EFM is a very powerful technique to study different physical properties of surfaces. One of these modes, called scanning polarization force microscopy (SPFM) [2], probes the dielectric response of the surface in a non-contact regime, allowing the direct characterization of the surface of both liquids and solids. SPFM is used in combination with the more conventional Kelvin probe microscopy (KPM) [3, 4] to obtain simultaneously information about surface charge distribution. In spite of the possibilities offered by the combination of these two techniques, the information related to the surface potential obtained by KPM mode has been exploited but only to a limited extent, due to the rather involved interpretation of KPM images [5]. However, the relevant information associated with the dielectric response of the surface is much less explored [6], in part because of the convolution of such a contribution with surface topography [7].

In this work we present a technique to measure the contribution of the dielectric response to the SPFM signal. We employ the generalized image charge method (GICM) to numerically simulate the electrostatic interaction between the EFM tip and the surface under study and show that a knowledge of the tip geometry is crucial. To demonstrate this we analyze the experimental SPFM signal for a system that consists of a few-layer graphene sheet on a silicon surface. Graphene, nowadays an extensively studied system because of its remarkable physical properties, namely its high carrier mobility [8], its control on the electronic structure [9] and the possibility to tune the density and type of carriers [10], is a truly two-dimensional single crystal of carbon atoms arranged in a honeycomb lattice [11]. The structural and electric properties of graphene make it a promising candidate as a building block for a novel generation of nanoelectronic devices [12–14]. We have chosen such a system because both materials are rather flat, stable in ambient conditions and

because of their huge difference in dielectric constants. An important outcome of the present work is that, in order to extract relevant physical information from the obtained images, the *macroscopic* shape of the tip, rather than the nanoscopic shape of the tip apex, has to be considered, due to the long-range nature of the electrostatic forces. Although it is already well known that the detailed shape of the tip must be taken into account for a precise quantitative analysis of the electrostatic forces [15], simplified models approximating the tip by a sphere have been widely successfully used [2, 16]. In this study we show that such simplified models are completely insufficient to reproduce the observed images when materials with clearly differentiated dielectric response are involved.

2. Experiments

All the experiments shown here were carried out at room temperature with an Agilent 5500 atomic force microscope (Agilent Technologies, Santa Clara, USA). This AFM has been home modified to operate in the SPFM mode. Commercial soft rectangular silicon cantilevers coated with a ≈25 nm platinum–iridium–chromium film (PPP-CONTPt, Nanosensors, Neuchâtel, Switzerland) were used for SPFM and contact experiments. Such cantilevers had a nominal spring constant of ∼0.5 N m^{-1} and a resonance frequency of ∼13 kHz. SPFM experiments were performed at 4 kHz oscillation frequency, thus well below the cantilever resonance. The microscope head was enclosed in a glove box to control the environment. Humidity control was achieved by circulating dry N_2 to decrease relative humidity (RH). All experiments where performed under low humidity conditions (RH < 10%). Working in a low humidity environment is crucial since it is known that the electrostatic properties of the SiO_2 surface [17] and the graphene films [18] are very sensitive to RH. In addition, the measurements can become strongly unstable by the formation of a water neck meniscus between the tip and the sample, especially when electric fields are present [19].

Few-layer graphene (FLG) films on silicon wafers were prepared using the conventional micromechanical exfoliation technique [12], where a flake of bulk Kish graphite is repeatedly cleaved with an adhesive tape and pressed down onto a silicon wafer coated with 280 nm thermally grown silicon oxide. Standard wafer protection tape for microfabrication by ICROS was used.

3. Theory

To perform SPFM, a conductive tip is brought about 10–20 nm above the sample surface and electrically biased to a few volts, creating attractive electrostatic forces between the tip and the polarizable surface. The external voltage applied to the tip is of the form

$$V_{\mathrm{tip}} = V_{\mathrm{dc}} + V_{\mathrm{ac}} \sin(\omega t), \tag{1}$$

where V_{dc} and V_{ac} correspond to the dc and ac voltages, respectively, and ω to the oscillation frequency. Assuming parallel-plate capacitor geometry for the tip–sample system, the force sensed by the tip can be expressed by [4]

$$F = -\frac{1}{2}\frac{\partial C}{\partial z}(V_{\mathrm{tip}} - \phi)^2 \tag{2}$$

where C and ϕ stand for the capacitance and the local contact potential difference between the tip and the sample, respectively, and z represents the direction perpendicular to the surface. Expanding equation (2) using equation (1), the following expressions for the ω and 2ω components are obtained:

$$F_{\omega} = -\frac{\partial C}{\partial z}\left[(V_{\mathrm{dc}} - \phi)V_{\mathrm{ac}} \sin(\omega t)\right] \tag{3}$$

$$F_{2\omega} = \frac{1}{4}\frac{\partial C}{\partial z}\left[V_{\mathrm{ac}}^2 \cos(2\omega t)\right]. \tag{4}$$

Two lock-in amplifiers are used to measure the $F(\omega)$ and $F(2\omega)$ forces experienced by the tip at the first and second harmonics, respectively. In SPFM the second harmonic term is used for feedback control. A feedback loop maintains the amplitude of the 2ω component of the lever oscillation constant by controlling the z piezodisplacement. It is important to emphasize that the $F(2\omega)$ term contains mixed information on topography and sample polarizability. Increases in sample polarizability on the sample are observed in the SPFM images as changes in apparent height due to the piezoretraction to compensate the increase of the electrostatic interaction between the tip and the sample. We make use of this property in the present work [7]. The first harmonic term $F(\omega)$ is proportional to the tip–sample contact potential difference (see equation (3)). A second feedback loop adjusts V_{dc} to null the $F(\omega)$ component, thus providing a direct measurement of the tip–surface contact potential difference as for the KPM technique.

4. Results

Figure 1(a) shows contact (top), SPFM (middle) and KPM (bottom) images of a few microns wide FLG sample. Several protrusions due to 3D folding of the FLG can be observed. From contact measurements of flat areas the FLG thickness H was estimated to be $H = 1.6 \pm 0.4$ nm. Assuming a graphite basal plane separation of ∼0.3–0.4 nm, this leads to an FLG formed of ∼5 layers. However, it has been recently reported that a single graphene layer can also exhibit 1.6 nm step heights due to the uncertain FLG–SiO_2 interfacial contribution (most probably due to water), since such samples are prepared in air [12]. Therefore, our sample could also consist of a single monolayer. The KPM image taken simultaneously with the SPFM image (figure 1(a), bottom) shows a contact difference potential slightly less positive in the FLG region as compared to the SiO_2 substrate, as has been already reported in the literature [20].

The SPFM image is an amplified replica of the topography of the FLG film obtained from the contact image (see profiles in figure 1(b)). We are even able to observe some of the larger protrusions observed in the contact image. This fact

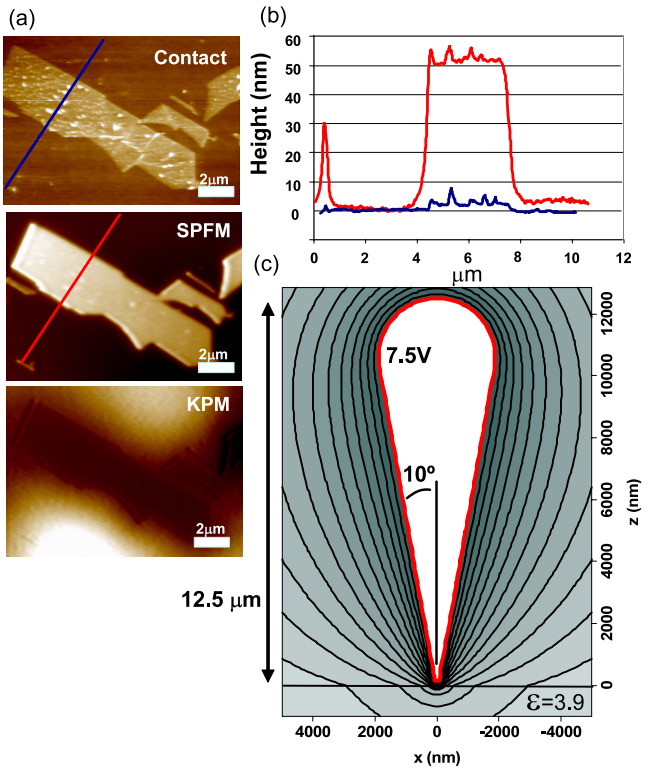

Figure 1. (a) Contact (top), SPFM (middle) and KPM (bottom) images taken for an FLG film transferred onto a SiO_2 surface. (b) Measured height for both contact (blue, upper) and SPFM (red, lower) images. (c) Generalized image charge method simulation of the electrostatic potential including the nominal macroscopic shape of the tip: $R = 50$ nm, $V = 7.5$ V, $\theta = 10°$ and $L = 12\,500$ nm.

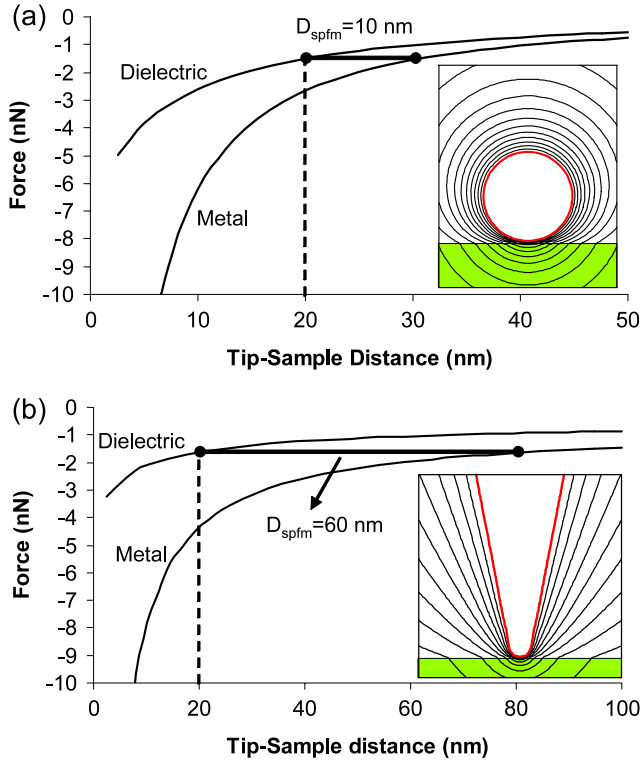

Figure 2. Simulations of the electrostatic force for both a metallic ($\varepsilon \sim \infty$) and dielectric ($\varepsilon = 3.9$) sample for a spherical ($R = 50$ nm) (a) and a macroscopic ($R = 50$ nm, $\theta = 10°$ and $L = 12\,500$ nm) tip (b). The SPFM displacement for $D = 20$ nm is shown in both figures. In both cases $V = 7.5$ V.

indicates that the loss of resolution due to the higher tip–sample distance [21] in SPFM, evaluated in the 10–20 nm range, has a minor effect for images of this size. Note the large difference in the height between contact (1.6 nm) and SPFM (50 nm) images. This difference in the measured thickness is due to the fact that in SPFM differences in $F(2\omega)$ ($\partial C/\partial z$ term in equation (4)) include the contributions from both the topography and the dielectric constant of the sample. The different dielectric constant between the FLG ($\varepsilon \sim \infty$) and SiO_2 ($\varepsilon = 3.9$) becomes the main contribution to the measured thickness. We point out the importance of using homogeneous planar surfaces in order to correctly characterize the actual topographic height.

5. Discussion

To quantify the large difference between the SPFM signal and the topography, we have simulated the electrostatic interaction with the generalized image charge method [22] (GICM). The GICM is based on the replacement of the tip by a set of point charges and segments that are adjusted in order to keep the electrostatic potential constant over the tip surface. The electrostatic force (and force gradient) can be obtained directly from the interaction of the charges inside the tip with their images or from the derivative of the capacitance C with respect to the tip–sample distance since $F \propto \partial C/\partial z$. One of the main advantages of this method is that macroscopic elements such as the sample or the cantilever can be included in the simulation by a series of image charges [23]. As reported before, the GICM is able to deal with distances between a few nanometers for the tip–sample distance D and several microns for the tip length L [24]. This characteristic can be used to analyze the influence of the macroscopic shape of the tip in the SPFM signal. To simulate the tip, we have considered a generic tip with a half-angle $\theta = 10°$, $L = 12.5$ μm, tip radius R between 50 and 200 nm and an applied voltage $V = 7.5$ V (see figure 1(c)).

In figure 2 we show the electrostatic force F as a function of D for both FLG and SiO_2. Following the asymptotic potential approach [25] and taking into account that the thickness of SiO_2 is almost an order of magnitude smaller than the tip length, FLG is approximated for simplicity by a semi-infinite metallic sample. In this case, the voltage on the graphene is nearly the same as the one on the Si backgate, which is grounded during the experiment. Moreover, its large size compared to the tip prevents the electric field from penetrating in SiO_2, which is located below. SiO_2 was included in the simulation as a semi-infinite dielectric sample with $\varepsilon = 3.9$. To estimate the SPFM displacement (D_{SPFM}) we focus on a fixed D for SiO_2 and calculate the distance that would give the same force over the FLG. For clarity, we have explicitly shown this process in figure 2 for $D = 20$ nm.

As depicted from figure 2(a), D_{SPFM} for a spherical tip lies below 10 nm. However, figure 2(b) shows that the contrast for a

macroscopic tip with the same R can be increased up to 60 nm, in good agreement with the experimental values shown in figure 1. This large difference is due to the slower convergence that the F versus D curve suffers for a macroscopic tip over a metallic sample when D increases. Due to the long-range nature of the electrostatic force, the very high mutual polarization between the FLG (metal) and the macroscopic shape of the tip is felt at distances as large as $D = 100$ nm. Focusing on the differences in the contrast values between the spherical and macroscopic tip, we conclude that the main contribution to the SPFM contrast is essentially due to the macroscopic shape of the tip and to a limited extent to the shape of tip apex.

Figure 3 shows calculated D_{SPFM} values for $R = 50$, 100, 150 and 200 nm compared to measured D_{SPFM} values as a function of D. Below 12 nm tip–sample distance the operation in the SPFM mode becomes unstable, even at low humidity, with the risk of snapping to contact. Although the GICM is optimized for including differences of several orders of magnitude in the simulations, it cannot accurately simulate tip radii below 50 nm due to the large difference with the tip length (12 500 nm). Although direct comparison cannot be made between theory and experiments, we can observe that the experimental values are placed in the lower limit of the curves, which correspond to the lowest values of the tip radii (SEM images gave $R = 25 \pm 5$ nm for the tips of the batch used in the experiments). On the other hand, the difference between theory and experiments for large values of D is the result of the increasing contribution of the conducting cantilever to the SPFM signal, which becomes more important at larger distances due to the decreasing contribution from the tip. The large dimension of the cantilever (30 μm wide) compared with the graphene (4 μm wide, see figure 1) means that at any time during the measurements part of the cantilever is on top of the graphene and part of it is on top of the SiO_2 substrate, and thus the contribution of the cantilever to the image is a convolution of both interactions. This effect might be reduced by reducing the dielectric constant of the cantilever side exposed to the sample while preserving the metallic conductivity of the tip and cantilever (i.e. metallic coating on the detector side), having in mind the need for using low force constant cantilevers, ideally <1 N m^{-1}, in order to enhance the force sensitivity. Such technical improvements are being considered as a future work.

As we can see in figure 3, D_{SPFM} is an almost linear function of D for all the tip radii. A good knowledge of D could be used to estimate the effective electrostatic tip radius [26]. Moreover, as shown recently, results from figures 2 and 3 could be also combined with artificial neural networks to simultaneously estimate D and the effective electrostatic tip radius [27]. The relevance of the tip radius and shape shown in figures 2 and 3 is in good agreement with previous works [24, 28–30] where the electrostatic signal in different setups (electrostatic force microscopy, Kelvin probe force microscopy, non-contact atomic force microscopy, scanning capacitance microscopy, ...) has been analyzed. Although the electrostatic force always depends on the tip geometry when the sample is dielectric, its influence in the final image strongly depends on the microscope setup [29]. Using the results shown in figures 2 and 3, we can quantitatively compare the influence of the macroscopic shape of the tip and the tip apex in SPFM. As we show in figure 2, the macroscopic shape of the tip makes the SPFM contrast six times bigger than that of a spherical tip with the same radius. If figure 3, however, the numerical simulations show that changes in the tip radius have a much smaller effect. For example, focusing on the smallest tip–sample distance in figure 3 (2.5 nm), the SPFM contrast takes values between 27 and 67 nm for tip radii between 50 and 200 nm. A four times bigger tip radius only doubles the contrast. This effect is much smaller than the one shown in figure 2 (six times bigger) due to the macroscopic shape of the tip.

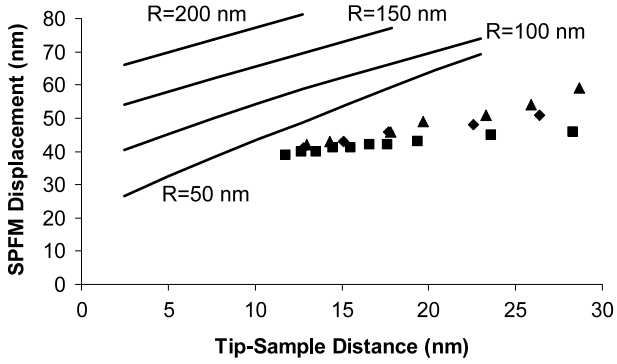

Figure 3. Simulated SPFM displacements compared with experimentally determined displacements as a function of the tip–sample distance. The experimental points correspond to three different measurements made in different sessions. Scanning electron microscopy images of the brand new tips gave a tip radius of $R = 25 \pm 5$ nm.

6. Conclusions

In conclusion, we have found a large contrast in SPFM images of FLG transferred onto a SiO_2 surface due to the differences in dielectric response. Using the generalized image charge method, we have shown that the macroscopic shape of the tip must be included in the simulations to quantitatively reproduce the experimental SPFM images. More than this, the main contribution to the SPFM comes from the macroscopic shape instead of from the tip apex. From the theoretical simulations, we have found a quasi-linear dependence of the SPFM tip displacement with the tip–sample distance. This simple relation can be used to estimate the SPFM working tip–sample distance and/or the effective electrostatic tip radius.

Acknowledgments

This work was supported by the Ministerio de Educación y Ciencia (MEC), Spain, through project FIS2006-12117-C04-01, from Explora program NAN2007-29375-E and by Generalitat de Catalunya (SGR 00909). AV acknowledges support from the Spanish Ramón y Cajal Program, MEC.

References

[1] Martin Y, Abraham D W and Wickramasinghe H K 1988 *Appl. Phys. Lett.* **52** 1103
[2] Hu J, Xiao X D and Salmeron M 1995 *Appl. Phys. Lett.* **67** 476
[3] Nonnenmacher N, O' Boyle M P and Wickramasinghe H K 1991 *Appl. Phys. Lett.* **58** 2921
[4] Samorì P (ed) 2006 *Scanning Probe Microscopies Beyond Imaging* (Weinhaim: Wiley–VCH)
[5] Charrier D S H, Kemerink M, Smalbrugge B E, de Vries T and Janssen R A J 2008 *ACS Nano* **2** 622
[6] Crider P S, Majewski M R, Zhang J, Oukris H and Israeloff N E 2007 *Appl. Phys. Lett.* **91** 013102
[7] Gómez-Moñivas S, Sáenz J J, Carminati R and Greffet J J 2000 *Appl. Phys. Lett.* **76** 2955
[8] Novoselov K S *et al* 2005 *Nature* **438** 197
[9] Ohta T, Bostwick A, Seyller T, Horn K and Rotenberg E 2006 *Science* **313** 951
[10] Zhang Y, Tan Y-W, Stormer H and Kim P 2005 *Nature* **438** 201
[11] Geim A K and Novoselov K S 2007 *Nat. Mater.* **6** 183
[12] Schedin F 2007 *Nat. Mater.* **6** 652
[13] Williams J R, Di Carlo L and Marcus C M 2007 *Science* **317** 638
[14] Novoselov K S, Geim A K, Morozov S V, Jiang D, Zhang Y, Dubonos S V, Grigorieva I V and Firsov A A 2004 *Science* **306** 666
[15] Watanabe S, Hane K, Ohye T, Ito M and Goto T 1993 *J. Vac. Sci. Technol.* B **11** 1774
[16] Verdaguer A, Cardellach M and Fraxedas J 2008 *J. Chem. Phys.* **129** 174705
[17] Verdaguer A, Weis C, Oncins G, Ketteler G, Bluhm H and Salmeron M 2007 *Langmuir* **23** 9699
[18] Moser J, Verdaguer A, Jiménez D, Barreiro A and Bachtold A 2008 *Appl. Phys. Lett.* **92** 123507
[19] Sacha G M, Verdaguer A and Salmeron M 2006 *J. Phys. Chem.* B **110** 14870
[20] Datta S S, Strachan D R, Mele E J and Charlie Johnson A T 2009 *Nano Lett.* **9** 7
[21] Gómez-Moñivas S, Froufe L S, Carminati R, Greffet J J and Sáenz J J 2001 *Nanotechnology* **12** 496
[22] Sacha G M, Sahagún E and Sáenz J J 2007 *J. Appl. Phys.* **101** 024310
[23] Sacha G M, Gómez-Navarro C, Sáenz J J and Gómez-Herrero J 2006 *Appl. Phys. Lett.* **89** 173122
[24] Gómez-Moñivas S, Froufe-Pérez L S, Caamaño A J and Sáenz J J 2001 *Appl. Phys. Lett.* **79** 4048
[25] Sacha G M and Sáenz J J 2004 *Appl. Phys. Lett.* **85** 2610
[26] Sacha GM, Verdaguer A, Martínez J, Sáenz J J, Ogletree D F and Salmeron M 2005 *Appl. Phys. Lett.* **86** 123101
[27] Sacha G M, Rodríguez F B and Varona P 2009 *Nanotechnology* **20** 085702
[28] Zerweck U, Loppacher C, Otto T, Grafstrom S and Eng L M 2005 *Phys. Rev.* B **71** 125424
[29] Sadewasser S, Carl P, Glatzel T and Lux-Steiner M C 2004 *Nanotechnology* **15** S14
[30] Sacha G M and Sáenz J J 2008 *Phys. Rev.* B **77** 245423